

Discrete-like diffraction dynamics in free space

Armando Perez-Leija,^{1,*} Francisco Soto-Eguibar,² Sabino Chavez-Cerda,²
Alexander Szameit,¹ Hector Moya-Cessa,^{2,3} and Demetrios N. Christodoulides³

¹*Institute of Applied Physics, Abbe Center of Photonics, Friedrich-Schiller-Universität Jena, Max-Wien-Platz 1, 07743 Jena, Germany*

²*Instituto Nacional de Astrofísica, Óptica y Electrónica, Coordinación de Óptica, Calle Luis Enrique Erro No. 1, 72840 Tonantzintla, Pue., Mexico*

³*CREOL/The College of Optics & Photonics, University of Central Florida, Orlando, Florida, USA*
armando.perez-leija@uni-jena.de

Abstract: We introduce a new class of paraxial optical beams exhibiting discrete-like diffraction patterns reminiscent to those observed in periodic evanescently coupled waveguide lattices. It is demonstrated that such paraxial beams are analytically described in terms of generalized Bessel functions. Such effects are elucidated via pertinent examples.

©2013 Optical Society of America

OCIS codes: (050.1940) Diffraction; (260.2030) Dispersion; (350.5500) Propagation.

References and links

1. D. N. Christodoulides, F. Lederer, and Y. Silberberg, "Discretizing light behaviour in linear and nonlinear waveguide lattices," *Nature* **424**(6950), 817–823 (2003).
2. H. Trompeter, T. Pertsch, F. Lederer, D. Michaelis, U. Streppel, A. Bräuer, and U. Peschel, "Visual Observation of Zener Tunneling," *Phys. Rev. Lett.* **96**(2), 023901 (2006).
3. S. Longhi, "Jaynes-Cummings photonic superlattices," *Opt. Lett.* **36**(17), 3407–3409 (2011).
4. R. Keil, A. Perez-Leija, P. Aleahmad, H. Moya-Cessa, S. Nolte, D. N. Christodoulides, and A. Szameit, "Observation of Bloch-like revivals in semi-infinite Glauber-Fock photonic lattices," *Opt. Lett.* **37**(18), 3801–3803 (2012).
5. R. Keil, A. Perez-Leija, F. Dreisow, M. Heinrich, H. Moya-Cessa, S. Nolte, D. N. Christodoulides, and A. Szameit, "Classical Analogue of Displaced Fock States and Quantum Correlations in Glauber-Fock Photonic Lattices," *Phys. Rev. Lett.* **107**(10), 103601 (2011).
6. A. Perez-Leija, R. Keil, A. Szameit, A. F. Abouraddy, H. Moya-Cessa, and D. N. Christodoulides, "Tailoring the Correlation and Anticorrelation behavior of Path-entangled Photons in Glauber-Fock Oscillator Lattices," *Phys. Rev. A* **85**(1), 013848 (2012).
7. M. Bellec, G. M. Nikolopoulos, and S. Tzortzakos, "Faithful communication Hamiltonian in photonic lattices," *Opt. Lett.* **37**(21), 4504–4506 (2012).
8. A. Rai and G. S. Agarwal, "Possibility of coherent phenomena such as Bloch oscillations with single photons via W states," *Phys. Rev. A* **79**(5), 053849 (2009).
9. Y. Lahini, A. Avidan, F. Pozzi, M. Sorel, R. Morandotti, D. N. Christodoulides, and Y. Silberberg, "Anderson Localization and Nonlinearity in One-Dimensional Disordered Photonic Lattices," *Phys. Rev. Lett.* **100**(1), 013906 (2008).
10. A. Peruzzo, M. Lobino, J. C. F. Matthews, N. Matsuda, A. Politi, K. Poullos, X. Q. Zhou, Y. Lahini, N. Ismail, K. Wörhoff, Y. Bromberg, Y. Silberberg, M. G. Thompson, and J. L. O'Brien, "Quantum Walks of Correlated Photons," *Science* **329**(5998), 1500–1503 (2010).
11. Y. Bromberg, Y. Lahini, and Y. Silberberg, "Bloch Oscillations of Path-Entangled Photons," *Phys. Rev. Lett.* **105**(26), 263604 (2010).
12. J. C. F. Matthews, K. Poullos, J. D. A. Meinecke, A. Politi, A. Peruzzo, N. Ismail, K. Wörhoff, M. G. Thompson, and J. L. O'Brien, "Simulating quantum statistics with entangled photons: a continuous transition from bosons to fermions," Preprint: arXiv:1106.1166.
13. A. Perez-Leija, R. Keil, A. Kay, H. Moya-Cessa, S. Nolte, L. C. Kwek, B. M. Rodríguez-Lara, A. Szameit, and D. N. Christodoulides, "Coherent quantum transport in photonic lattices," *Phys. Rev. A* **87**(1), 012309 (2013).
14. A. Perez-Leija, R. Keil, H. Moya-Cessa, A. Szameit, and D. N. Christodoulides, "Perfect transfer of path-entangled photons in 1D photonic lattices," *Phys. Rev. A* **87**(2), 022303 (2013).
15. F. Dreisow, A. Szameit, M. Heinrich, T. Pertsch, S. Nolte, and A. Tünnermann, "Second-order coupling in femtosecond-laser-written waveguide arrays," *Opt. Lett.* **33**(22), 2689–2691 (2008).
16. A. Szameit, T. Pertsch, S. Nolte, A. Tünnermann, and F. Lederer, "Long-range interaction in waveguide lattices," *Phys. Rev. A* **77**(4), 043804 (2008).
17. A. L. Jones, "Coupling of optical fibers and scattering fibers," *J. Opt. Soc. Am.* **55**(3), 261 (1965).
18. G. Dattoli, L. Giannessi, L. Mezi, and A. Torre, "Theory of generalized Bessel functions," *Nuovo Cim.* **105**(3), 327–348 (1990).
19. G. Dattoli, A. Torre, S. Lorenzutta, and G. Maino, "Theory of generalized Bessel functions II," *Nuovo Cim.* **106**(1), 21–51 (1991).

20. J. C. Gutiérrez-Vega and M. A. Bandres, "Helmholtz-Gauss waves," *J. Opt. Soc. Am. A* **22**(2), 289–298 (2005).
21. J. M. Zeuner, N. K. Efremidis, R. Keil, F. Dreisow, D. N. Christodoulides, A. Tünnermann, S. Nolte, and A. Szameit, "Optical Analogues for massless Dirac particles and conical diffraction in one dimension," *Phys. Rev. Lett.* **109**(2), 023602 (2012).
21. N. K. Efremidis and D. N. Christodoulides, "Abruptly autofocusing waves," *Opt. Lett.* **35**(23), 4045–4047 (2010).
22. N. K. Efremidis, P. Zhang, Z. Chen, D. N. Christodoulides, C. E. Ruter, and D. Kip, "Wave propagation in waveguide arrays with alternating positive and negative couplings," *Phys. Rev. A* **81**(5), 053817 (2010).
23. N. K. Efremidis and D. N. Christodoulides, "Abruptly autofocusing waves," *Opt. Lett.* **35**(23), 4045–4047 (2010).
24. J. W. Goodman, *Introduction to Fourier Optics*, McGraw-Hill Physical and Quantum Electronics Series (Roberts, 2005).
25. H. Moya-Cessa and F. Soto-Eguibar, *Differential Equations: An Operational Approach* (Rinton Press, 2011).
26. C. Gerry and P. L. Knight, *Introductory Quantum Optics* (Cambridge, 2005).
27. W. H. Louisell, *Quantum and Statistical Properties of Radiation* (Wiley, 1973).

1. Introduction

The ability to tailor and manipulate the dynamics of classical and non-classical light using photonic lattices has become a topic of importance for scientific research and practical applications [1]. As it has been shown in a number of studies, such discrete optical arrangements can be pre-engineered in order to produce discrete wave dynamics similar to those occurring in diverse branches of physics [2–9]. For instance, optical fields traversing one-dimensional periodic lattices undergo discrete diffraction and as a result they evolve in a way entirely analogous to electronic wave-functions in crystalline structures [1]. In this respect, the effective discretization of the underlying field dynamics allows one to observe the corresponding electron states within the realm of optics [8]. Meanwhile, in quantum optics, such discretization of the wave-functions has been exploited in order to carry out several interesting investigations such as quantum walks of correlated photons [10], Bloch oscillations of NOON states [11], simulations of different quantum statistics [12], and the perfect transfer of quantum states [13, 14].

Evidently, devising new schemes capable of extending the concept of discrete diffraction in other settings is of high importance. Of particular interest will be to realize such discrete diffraction patterns even in the absence of a periodic environment, e.g. in the bulk of a uniform material or even in free space. In this paper we demonstrate that paraxial optical beams exhibiting discrete-like diffraction patterns are possible in homogeneous media that are reminiscent to those encountered in periodic evanescently coupled waveguide lattices endowed with coupling interactions up to second order. The evolution of such paraxial beams are analytically described in terms of generalized Bessel functions. The prospects of observing these effects are also discussed.

2. Theoretical analysis

As previously mentioned, this new class of paraxial optical beams introduced here, can exhibit discrete-like diffraction patterns resembling those arising from the impulse response (single site excitation) in periodic photonic lattices with first and second order interaction couplings, (see Figure 1) [15, 16]. We show that such paraxial beams can be produced after propagating a field profile having the form of a Bessel function of integer order. For implementation purposes, we also assume that this Bessel field distribution is apodized in a Gaussian manner. In other words, the initial field profile is given by $\psi(s, \xi = 0) = \exp(-s^2/2\sigma^2)J_n(\alpha s)$, where $s \in (-\infty, \infty)$ and ξ represent normalized transverse and longitudinal coordinates, respectively. Interestingly, the propagation dynamics obeyed by such optical beams can be described in closed form, from where one can analytically predict their ballistic-like behavior.

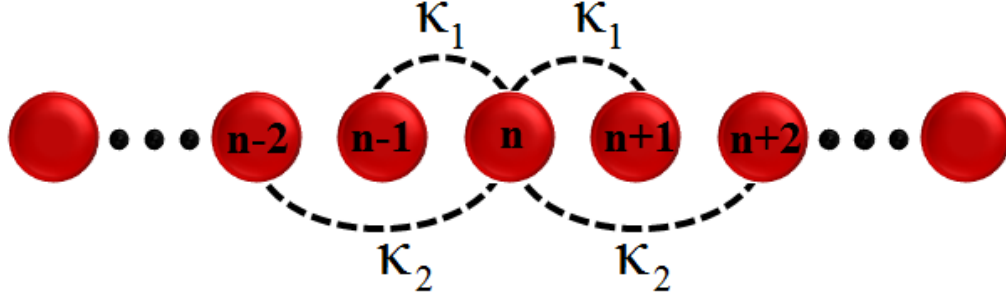


Fig. 1. Transverse view of an array of evanescently coupled single mode waveguides. κ_1 is the coupling strength between nearest neighbors whereas κ_2 represents the couplings between next-nearest neighbors.

For comparison purposes, we start by briefly reviewing the optical dynamics observed in periodic one-dimensional arrays of evanescently coupled single-mode waveguides having first and second order coupling interactions. To this end, we employ the coupled-mode formalism, where the transverse profiles of the propagating modes are assumed to remain invariant and only the amplitudes evolve along the direction of propagation [16]. Accordingly, the mode amplitude at the m^{th} waveguide is governed by the set of coupled differential equations

$$i \frac{dE_m}{dZ} + \kappa_1 (E_{m+1} + E_{m-1}) + \kappa_2 (E_{m+2} + E_{m-2}) = 0, \quad (1)$$

where $m \in (-\infty, \infty)$, Z is the normalized propagation distance, κ_1 represents the coupling coefficient between the m^{th} element and its nearest neighbors, whereas κ_2 stands for second order interactions. In this case, one can show that the field amplitude at waveguide m when light is launched into the 0-th channel is given by

$$E_m(Z) = \sum_{l=-\infty}^{\infty} i^{m-l} J_{m-2l}(2\kappa_1 Z) J_l(2\kappa_2 Z), \quad (2)$$

where $J_m(Z)$ is the Bessel function of the first kind and order m [16]. By using the identity $J_m(x, y; r) = \sum_{l=-\infty}^{\infty} r^l J_{m-2l}(x) J_l(y)$, where $J_m(x, y; r)$ represents a generalized Bessel function (GBF) of order m [18, 19], Eq. (2) can be written in a more compact form

$$E_m(Z) = i^m J_m(2\kappa_1 Z, 2\kappa_2 Z; -i). \quad (3)$$

Note that a GBF of order m can be computed through the finite integral

$$J_m(x, y; 1) = \frac{1}{2\pi} \int_{-\pi}^{\pi} \exp[i(x \sin(\phi) + y \sin(2\phi) - m\phi)] d\phi,$$

when $r = 1$, and they obey the recurrence relations

$$2mJ_m(x, y; r) = x[J_{m-1}(x, y; r) + J_{m+1}(x, y; r)] + 2y \left(rJ_{m-2}(x, y; r) + \frac{1}{r}J_{m-2}(x, y; r) \right),$$

and have the generating function [18]

$$T(x, y; r, t) = \sum_{m=-\infty}^{\infty} t^m J_m(x, y; r) = \exp\left(\frac{x}{2}\left(t - \frac{1}{t}\right) + \frac{y}{2}\left(rt^2 - \frac{1}{rt^2}\right)\right).$$

We now turn to the analysis of the paraxial propagation dynamics of Bessel field distributions of the form $\psi(s, \xi=0) = \exp(-s^2/2\sigma^2)J_n(\alpha s)$. We first study the case when the initial field can be written as a product of two arbitrary functions in the transverse coordinate, that is, $\psi(s, \xi=0) = g(s)f(s)$. The choice of this type of initial condition is quite natural since in practice one generally has to apply an apodizing function to the initial field profile, see for example [20]. In order to analyze this general case, we consider the normalized paraxial equation of diffraction

$$i \frac{\partial \psi}{\partial \xi} = -\frac{1}{2} \frac{\partial^2 \psi}{\partial s^2}, \quad (4)$$

where ψ is the electric field envelop, $\xi = z/kx_0^2$, $k = 2\pi n/\lambda_0$ is the wavenumber of the optical field, and $s = x/x_0$ represents a dimensionless transverse coordinate and x_0 is an arbitrary transverse scale. The solution for the paraxial Eq. (4) is given by

$$\psi(s, \xi) = \int_{-\infty}^{\infty} \int_{-\infty}^{\infty} F(w-u)G(u) \exp\left(i \frac{\xi}{2} w^2\right) \exp(isw) du dw. \quad (5)$$

The details of this reduction and subsequent solutions are given in the Appendix. On the other hand, for the case where the initial field is given by the product of an apodizing Gaussian profile and an arbitrary function $f(s)$, the propagated field is described by

$$\psi(s, \xi) = \exp(g_1 s^2 - i g_2) \int_{-\infty}^{\infty} F(v) \exp\left(i \left(\frac{\xi}{2} + g_3\right) v^2\right) \exp(isv \exp(-i 2g_2)) dv, \quad (6)$$

where $g_1(\xi) = -(2(\sigma^2 - i\xi))^{-1}$, $g_2(\xi) = -i \ln((\sigma^2 - i\xi)/\sigma^2)/2$, $g_3(\xi) = -\xi^2/2(\sigma^2 - i\xi)$. For the particular case where the initial field distribution is given by the functions $g(s) = \exp(-s^2/2\sigma^2)$ and $f(s) = J_n(\alpha s)$, Eq. (6) reduces to

$$\psi(s, \xi) = \frac{1}{2\pi} \exp(g_1(\xi)s^2 - i g_2(\xi)) \int_{-\pi}^{\pi} \exp(-in\phi + iA \sin(\phi) + iB \sin^2(\phi)) d\phi, \quad (7)$$

where $A(s) = (\alpha s \sigma^2 / (\sigma^2 - i\xi))$, $B(\xi) = \alpha^2 \left[\frac{\xi}{2} - i g_3(\xi) \right]$. After some algebra, as indicated in the Appendix, Eq. (7) can be cast as follows

$$\psi(s, \xi) = \exp\left(g_1(\xi)s^2 - i \left(g_2(\xi) - \frac{B}{2}\right)\right) \sum_{m=-\infty}^{\infty} (-i)^m J_{n+2m}(A) J_m(B/2). \quad (8)$$

Note that Eq. (8) can be expressed in terms of the GBF of order n using the identity $J_n(A, B/2; -i) = \sum_{m=-\infty}^{\infty} (-i)^m J_{n+2m}(A) J_m(B/2)$. This in turn reveals the mathematical similitude between the impulse response of the aforementioned photonic lattices and the paraxial GBF beams studied here. A useful representation of the GBF is given by the finite

integral $J_n(x, y; r) = \frac{1}{2\pi} \int_{-\pi}^{\pi} \exp\left(\left[i\left(x \sin(\phi) - n\phi\right)\right]\right) \exp\left(\frac{y}{2} \left(r \exp(-i2\phi) - \frac{\exp(i2\phi)}{r}\right)\right) d\phi$. In

addition, for the numerical simulations presented here we found that taking into account 101 elements in the series given in Eq. (8), reproduce a solution with an error of 10^{-14} compared with the numerical integration of Eq. (4). By taking a closer look into the exponential terms accompanying the GBF in Eq. (8), one can see that the intensity dynamics is bounded by a modulating Gaussian envelope, $\exp\left(-(\sigma s)^2/(\sigma^4 + \xi^2)\right)$, which amplitude decreases along propagation as $\exp\left(-\alpha\sigma^2\xi^2/2(\sigma^4 + \xi^2)\right)/\sqrt{1+(\xi^2/\sigma^4)}$. Note that, as expected, at $\xi = 0$ the envelope becomes the intensity of the apodizing function, $\exp(-s^2/\sigma^2)$, whereas the series of Bessel functions collapses to $J_n(\alpha s)$. By comparing the series of Bessel functions appearing in Eq. (2) and Eq. (8), one can see that in the latter case the role of the first and second order interaction couplings are played by the complex functions $A(s)$ and $B(\xi)$, respectively. This fact introduces the possibility of inducing, in the present systems, complex-like “coupling coefficients”, something that on many occasions is desired in integrated waveguide arrays [22, 23]. At the same time, these complex arguments establish a limit for the observation of the discrete-like diffraction effects.

In what follows we show that discrete-like diffraction occurs as a result of the destructive and constructive interference undergone when left and right lobes of the initial field profile collide. This in turn impose a restriction to the possible values of σ , for instance, if we consider σ to be small enough such that by apodizing the initial Bessel function we truncate all the side lobes, then the propagating optical field will diffract in a way similar to a Gaussian beam. On the other hand, if σ is chosen to truncate just the higher order lobes, it will allows us to observe discrete- like diffraction. Furthermore, the qualitative effects in the diffraction process depend on the parity of the order of the initial Bessel functions, i.e., whether n is even or odd. To demonstrate this we compare the cases $n = 3$ and $n = 6$ for a beam propagating in free space and using the realistic parameters $\lambda_0 = 633\text{nm}$ and $x_0 = 10\mu\text{m}$. In Figs. 2(a), 2(b) and 2(c), 2(d), we present the calculated propagation dynamics corresponding to the initial field distributions $\psi(x, z=0) = \exp(-x^2/2\sigma^2)J_{3,6}(\alpha x)$. As clearly seen, in both cases the main lobes of the Bessel functions tend to propagate towards the center ($x=0$) and eventually collide after a certain propagation distance z . As a result, interference effects are observed within the “triangular region” subtended by the two highest energy branches. In fact, those two branches can be considered as the ballistic lobes for the paraxial beams examined here. Indeed such interference effects are responsible for the apparent discretization of the underlying optical fields. A notable difference between these two beams is the fact that whenever n is odd, an intensity gap is formed at exactly $x = 0$, (see Fig. 2(a)). This gap is a direct byproduct of the destructive interference caused by the π phase difference existing between the two sides ($-x$ and x) of the propagating optical $J_n(\alpha x)$ wave, and can also be readily explained from the analytical solution since $J_{2m+1}(0, y; r) = 0$. On the other hand, when n is even, the entire wave is in phase and as a result constructive interference takes place producing periodic peaks of intensity along the propagation axis at $x = 0$, that exactly follow a Bessel function since $J_{2m}(0, y; 1) = J_m(y)$, (see Fig. 2(c)). Note that in this latter case (n even), the optical field undergoes similar effects to those reported in reference [23] for autofocusing waves.

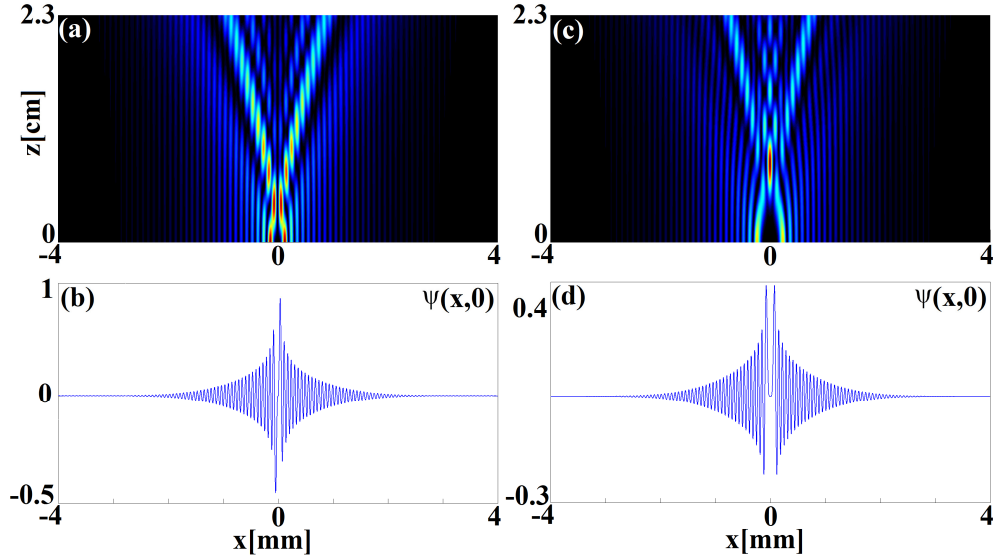


Fig. 2. (a) and (c) depict the intensity evolution of the initial fields $\psi(x,0) = \exp(-x^2/2\sigma^2)J_3(\alpha x)$ and $\psi(x,0) = \exp(-x^2/2\sigma^2)J_6(\alpha x)$, respectively. The parameters used are $\alpha=1$ and $\sigma=10^{-3}$. (b) and (d) show the corresponding initial field profile.

For the special case $n=0$, the situation is different and some special features are revealed. The most remarkable of them is that the field evolves in a way that is analogous to that expected in periodic photonic lattices, under single site excitations, when having couplings up to second order. In other words, the propagation dynamics exhibited in this particular case tends to spread out in a “ballistic” way, thus emulating in free space discrete diffraction phenomena. A suitable way to describe the dynamical evolution of wavepackets is through the average value of the transverse coordinate, $F(z) = \int \psi^*(x,z) x \psi(x,z) dx$, which in this case is proportional to z^2 , revealing so the ballistic nature of these waves. In Fig. (3) we illustrate these effects by comparing the intensity evolution of the initial field $\psi(x,z=0) = \exp(-x^2/2\sigma^2)J_0(\alpha x)$ (again using the parameters $\lambda_0 = 633\text{nm}$, $x_0 = 10\mu\text{m}$, $\alpha=1$ and $\sigma=10^{-3}$), Figs. 3 (a)-3(c), and the impulse response of a periodic photonic lattice containing 30 waveguide elements and coupling coefficients $\kappa_1 = 1\text{cm}^{-1}$ and $\kappa_2 = 0.1\text{cm}^{-1}$, Figs. 3 (d)-3(f). In order to elucidate the limitations of the proposed paraxial beams on the generation of discrete-like diffraction, in Fig. (4) we separately depict the intensity evolution of the same wavepacket $\psi(x,z=0) = \exp(-x^2/2\sigma^2)J_0(\alpha x)$, Fig. 4(a), and the Gaussian envelope, Fig. 4(b), for a longer propagation distance. In addition, to qualitatively demonstrate the ballistic spreading of the intensity, we have numerically computed the average value $F(z)$ on the semi-plane $x \in (-\infty, 0]$ (longitudinal yellow curve in Fig. (4)). Note that after the distance l , which gives the distance at which the average function $F(z)$ surpasses the point where the intensity of the envelope decays up to one-half of its maximum value (FWHM), the features of the discrete-like diffraction pattern start to disappear and completely vanish after $z=2l$. This is because after $z=l$, the imaginary part of the arguments $A(x)$ and $B(z)$ become dominant; this implies that after this particular distance,

the Bessel functions in the solution are proportional to $i^n I_n(r)$, where $I_n(r)$ represents the modified Bessel function. As a result, the arising modified Bessel functions tend to grow exponentially. However, since the GBFs are bounded by the Gaussian envelope, this exponential growing does not affect the physical meaning of the solution.

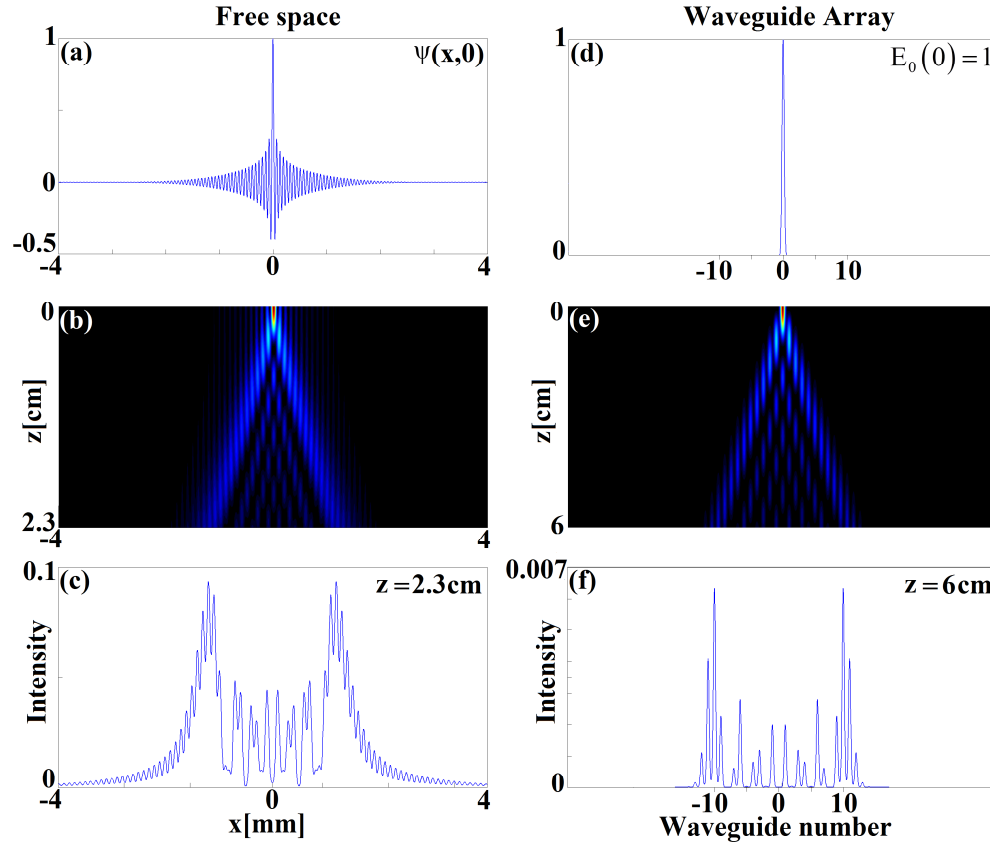


Fig. 3. Theoretical comparison of light propagation through free space for the initial field profile $\psi(x, 0) = \exp(-x^2/2\sigma^2)J_0(\alpha x)$ (a-c), and in a periodic photonic lattice of 30 elements, under a single site excitation (d-f). Figs. (a, d) depict the initial field distributions, (b, e) the normalized intensity evolution, and (c, f) the intensity profiles at the output. The parameters used for the paraxial beams are $\alpha = 1$ and $\sigma = 10^{-3}$. For the waveguide array we assumed coupling coefficients $\kappa_1 = 1 \text{ cm}^{-1}$ and $\kappa_2 = 0.1 \text{ cm}^{-1}$.

3. Conclusion

The theory developed in the present paper along with the numerical simulations clearly demonstrate the feasibility of generating discrete-like diffraction processes in free space by properly engineering the initial field profile. The implementation of these beams should be straightforward using a spatial light modulator in order to produce the proper amplitude and phase required by the initial field profiles. Our results can provide a new optical platform upon which one can study the effects of discrete diffraction over matter, like for example particles, molecules, etc.

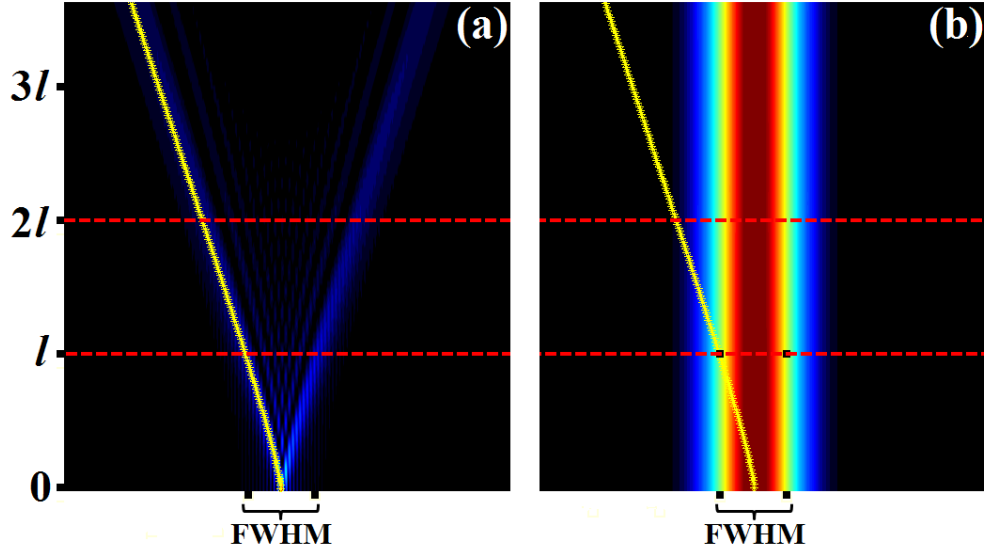


Fig. 4. (a) Intensity propagation of the field $\psi(x,0) = \exp(-x^2/2\sigma^2)J_0(\alpha x)$ and (b) the absolute square of the Gaussian envelope $\exp(-x^2/2\sigma^2)$, the parameters used are the same as in Fig. (3). In this case, we found that $FWHM = 3mm$, whereas $l = 3.3cm$.

4. Appendix

Starting from the normalized paraxial equation of diffraction $i\partial\psi/\partial\xi = -\partial^2\psi/2\partial s^2$, and defining the operator $p = -i\partial/\partial s$, such that the commutator $[s,p] = i$, it is clear that the formal solution to Eq. (4) is given by $\psi(s,\xi) = \exp(i\xi p^2/2)g(s)f(s)$. Then, expanding the product $f(s)g(s)$ in plane waves we obtain [24]

$$\psi(s,\xi) = \exp\left(i\frac{\xi}{2}\hat{p}^2\right) \int_{-\infty}^{\infty} G(u) \exp(isu) du \int_{-\infty}^{\infty} F(v) \exp(isv) dv. \quad (9)$$

By using the identity operator $\exp(-i\xi\hat{p}^2/2)\exp(i\xi\hat{p}^2/2) = 1$ and the Hadamard's lemma $\exp(i\xi\hat{p}^2/2)h(s)\exp(-i\xi\hat{p}^2/2) = h(s+\xi\hat{p})$ [23–25], Eq. (9) becomes

$$\psi(s,\xi) = \int_{-\infty}^{\infty} G(u) \exp(iu[s+\xi\hat{p}]) \exp\left(i\frac{\xi}{2}\hat{p}^2\right) du \int_{-\infty}^{\infty} F(v) \exp(isv) dv. \quad (10)$$

Since the commutator $[[\hat{p},s],\hat{p}] = [[\hat{p},s],s] = 0$, we can use the Baker-Hausdorff formula to split the exponential $\exp(iu[s+\xi\hat{p}]) = \exp(i\xi u^2/2)\exp(ius)\exp(i\xi u\hat{p})$ [25–27], so that Eq. (9) reduces to

$$\psi(s,\xi) = \int_{-\infty}^{\infty} G(u) \left(\int_{-\infty}^{\infty} F(v) \exp\left(\frac{i\xi u^2}{2}\right) \exp(ius) \exp(i\xi u\hat{p}) \exp\left(\frac{i\xi \hat{p}^2}{2}\right) \exp(isv) dv \right) du. \quad (11)$$

Using the fact that

$$\exp\left(\frac{i\xi\hat{p}^2}{2}\right)\exp(isv) = \sum_{k=0}^{\infty} \frac{(i\xi/2)^k}{k!} \left(-i\frac{\partial}{\partial s}\right)^{2k} \exp(isv) = \exp\left(\frac{i\xi v^2}{2}\right)\exp(isv) \quad (12)$$

and $\exp(i\xi\hat{p}u)\exp(isv) = \exp(i\xi uv)\exp(isv)$, Eq. (11) acquires the form

$$\psi(s, \xi) = \int_{-\infty}^{\infty} G(u) \left(\int_{-\infty}^{\infty} F(v) \exp\left(i\xi(u+v)^2/2\right) \exp(is(u+v)) dv \right) du \quad (13)$$

Then, by introducing the change of variable $w = u + v$ we obtain finally obtain Eq. (5)

$$\psi(s, \xi) = \int_{-\infty}^{\infty} G(u) \left(\int_{-\infty}^{\infty} F(w-u) \exp(i\xi w^2/2) \exp(isw) dw \right) du. \quad (14)$$

In order to obtain the field solution describing the propagation dynamics of the initial profile $\psi(s, \xi = 0) = \exp(-s^2/2\sigma^2)f(s)$, we start from the formal solution $\psi(s, \xi) = \exp(i\xi\hat{p}^2/2)\exp(-s^2/2\sigma^2)f(s)$. Again, after using the operator unitary identity $\exp(-i\xi\hat{p}^2/2)\exp(i\xi\hat{p}^2/2) = 1$ along with the transformation $\exp(i\xi\hat{p}^2/2)\exp(-s^2/2\sigma^2)\exp(-i\xi\hat{p}^2/2) = \exp(-(s^2 + \xi(sp + ps))\xi^2 p^2/2\sigma^2)$, the field solution can be expressed as

$$\psi(s, \xi) = \exp\left(-[s^2 + \xi(s\hat{p} + \hat{p}s) + \xi^2\hat{p}^2]/2\sigma^2\right) \exp(i\xi\hat{p}^2/2) f(s). \quad (15)$$

Since the operators $s^2, (s\hat{p} + \hat{p}s)$, and \hat{p}^2 provide an operator algebra, where the commutation relations between them are closed and given by: $[s^2, \hat{p}^2] = 2i(s\hat{p} + \hat{p}s)$, $[(s\hat{p} + \hat{p}s), \hat{p}^2] = i4\hat{p}^2$, and $[s^2, (s\hat{p} + \hat{p}s)] = i4s^2$, the first exponential can be factorized as follows

$$\exp\left(-\frac{[s^2 + \xi(s\hat{p} + \hat{p}s) + \xi^2\hat{p}^2]}{2\sigma^2}\right) = \exp(g_1(\xi)s^2) \exp(g_2(\xi)(s\hat{p} + \hat{p}s)) \exp(g_3(\xi)\hat{p}^2). \quad (16)$$

By differentiating both sides of Eq. (16) with respect to ξ , and using the commutation relations, one can show that $g_1(\xi) = -(2(\sigma^2 - i\xi))^{-1}$, $g_2(\xi) = -i \ln((\sigma^2 - i\xi)/\sigma^2)/2$, and $g_3(\xi) = -\xi^2/2(\sigma^2 - i\xi)$. Then, after using these functions along with Eq. (12), and expanding $f(s)$ in plane waves, the propagated field becomes

$$\psi(s, \xi) = \exp(g_1 s^2) \exp(g_2 (s\hat{p} + \hat{p}s)) \int_{-\infty}^{\infty} F(v) \exp\left(\left(i\frac{\xi}{2} + g_3\right)v^2\right) \exp(isv) dv. \quad (17)$$

Inserting the unitary operator identity $\exp(-g_2(s\hat{p} + \hat{p}s))\exp(g_2(s\hat{p} + \hat{p}s))$ after the term $\exp(isv)$ and using the fact that $\exp(g_2(s\hat{p} + \hat{p}s))1 = \exp(-ig_2)$, we obtain Eq. (6)

$$\psi(s, \xi) = \exp(g_1 s^2 - ig_2) \int_{-\infty}^{\infty} F(v) \exp\left(\left(i\frac{\xi}{2} + g_3\right)v^2\right) \exp(isv \exp(-i2g_2)) dv. \quad (18)$$

For the particular case where the initial field is a Bessel function of order n apodized by a Gaussian profile, $\psi(s, \xi = 0) = \exp(-s^2 / 2\sigma^2) J_n(\alpha s)$, we start from Eq. (15), and use the integral representation of Bessel functions $J_n(\alpha s) = \frac{1}{2\pi} \int_{-\pi}^{\pi} \exp(-i(n\phi - \alpha s \sin(\phi))) d\phi$. Then, following the same steps as in the previous case, one readily obtains Eq. (7)

$$\psi(s, \xi) = \frac{1}{2\pi} \exp(g_1 s^2 - i g_2) \int_{-\pi}^{\pi} \exp(-in\phi + iA \sin\phi + iB \sin^2 \phi) d\phi, \quad (19)$$

where $A = \alpha s \exp(-i2g_2(\xi))$ and $B = \alpha^2((\xi/2) - i g_3(\xi))$. By using the identity $\sin^2(\phi) = (1 - \cos(2\phi))/2$ and expanding the exponentials in Taylor series, Eq. (19) can be easily cast as

$$\psi(s, \xi) = \frac{1}{2\pi} \exp(g_1 s^2 - i(g_2 - B/2)) \sum_{j,m=0}^{\infty} \frac{1}{j!m!} \left(-\frac{iB}{4}\right)^{j+m} \int_{-\pi}^{\pi} \exp(-i(n+2j-2m)\phi + iA \sin\phi) d\phi \quad (20)$$

After some algebra and using the integral form of the Bessel function of the first kind, one can easily obtain Eq. (8).

Acknowledgments

HMC acknowledges support from Consejo Nacional de Ciencia y Tecnología (CONACyT), México and fruitful discussions with J.R. Moya-Cessa, E. Landgrave and V. Arrizon. The work of DNC was supported by the Air Force Office of Scientific Research (MURI Grant No. FA9550-10-1-0561) and the Israeli ministry of defense. The work of AS was supported by the German Ministry of Education and Research (Center of Innovations Competence program, grant no. 03Z1HN31) and the Thuringian Ministry of Education, Science and Culture, grant No. 11027-514.